ORIGINAL ARTICLE

Structural, functional, molecular, and biological evaluation of novel triterpenoids isolated from *Helichrysum stoechas* (L.) Moench. Collected from Mediterranean Sea bank: Misurata- Libya

Md. Sarfaraj Hussain [a,b,*], **Faizul Azam** [c], **Hanan Ahmed Eldarrat** [a], **Anzarul Haque** [d],
Mohammad Khalid [d], **Mohd. Zaheen Hassan** [e], **Mohammed Ali** [f], **Muhammad Arif** [g],
Irfan Ahmad [h], **Gaffar Zaman** [h], **Nadiyah M. Alabdallah** [i], **Mohd. Saeed** [j]

[a] *Department of Pharmacognosy, Faculty of Pharmacy, Misurata University, Misurata, Libya*
[b] *Lord Buddha Koshi Pharmacy College, Baijanathpur, Saharsa 852201, Bihar, India*
[c] *Department of Pharmaceutical Chemistry and Pharmacognosy, Unaizah College of Pharmacy, Qassim University, Unaizah 51911, Saudi Arabia*
[d] *College of Pharmacy, Department of Pharmacognosy, Prince Sattam Bin Abdul Aziz University, Al Kharj, Saudi Arab*
[e] *Department of Pharmaceutical Chemistry, College of Pharmacy, King Khalid University, Abha, Saudi Arabia*
[f] *Department of Pharmacognosy & Phytochemistry, Faculty of Pharmacy, Hamdard University, New Delhi, India*
[g] *Faculty of Pharmacy, Integral University, Kursi Road, Lucknow, India*
[h] *Department of Clinical Laboratory Sciences, College of Applied Medical Sciences, King Khalid University, P.O. Box 61413, Abha 9088, Saudi Arabia*
[i] *Department of Biology, College of Science, Imam Abdulrahman Bin Faisal University, P.O. Box 1982, 31441 Dammam, Saudi Arabia*
[j] *Department of Biology, College of Sciences, University of Hail, Hail, Saudi Arabia*

Abstract *Helichrysum stoechas* (L.) Moench (Family Compositae) is a medicinal herb endowed with several pharmacological activities. Ethanolic extract of the aerial parts of the plant was used for the isolation of lignoceric acid (HS-02), lanost-5- en-3β-ol- 26-oic acid (HS-03), and lanost-5-en-26-oic acid-3β-olyl palmitate (HS-04). All molecules were screened for anti-inflammatory and analgesic activities at 5 and 10 mg/kg body weight doses, and the TEST program assessed their toxicity.

* Corresponding author at: Department of Pharmacognosy, Faculty of Pharmacy, Misurata University, Misurata, Libya.
E-mail address: sarfarajpharma@gmail.com (Md. Sarfaraj Hussain).
Peer review under responsibility of King Saud University.

The molecular interaction profile with numerous anti-inflammatory drug targets was investigated by molecular docking. Compounds HS-03 and HS-04 showed a significant reduction in paw volume compared to the control group challenged with carrageenan in the rats, and prolongation of the paw licking/jumping and reduction in the number of writhes was noted after the injection of acetic acid in mice. In a hot plate test, all compounds showed significant pain inhibition. These findings might aid in the development of anti-inflammatory and anti-analgesic therapies.

1. Introduction

Natural medicinal plants are utilized for medicinal purposes for centuries and persist to be a medicine for various diseases even with the dramatic rise in antibiotics and other synthetic medicine within the current scientific world (Hussain et al., 2009, 2016, 2019, 2020a). *Helichrysum stoechas* (L.) Moench, syn. *Gnaphalium citrinum* Lam. and *G. stoechas* L. (Family Compositae), referred to as shrubby everlasting, God's flower, Gold flower, Golden stoechas, and Goldylocks, is common within the Mediterranean region, north-western Africa, eastern Turkey, southern India, Sri Lanka, and Australia on crude land and alongside the road. This plant better grows on soils with acidic, neutral, or basic pH and very much depleted sites (Hussain et al., 2020b; Tutin et al., 1980; Giuliani et al., 2016; Sobhy and El-Feky, 2007). The plant is perennial, evergreen, rugged, spreading, fragrant spice, growing up to 60 cm; with woolly stem, simple leaves, alternate, linear, with entire margins; flowers umbels of yellow many-stellate foliage. It has anti-inflammatory, antifungal and antioxidant, deobstruent, expectorant, laxative, and sudorific properties; used to treat hypersensitivities, bronchitis, normal colds, influenza, respiratory issues, and sinusitis. The aerial parts of the plant are commonly used as condiments for cooking soups, rice and meat dishes. Its volatile oil has healing, anti-aging, anti-inflammatory, hemostatic, lipolytic, and regenerating properties. The flowers are taken as a diaphoretic and discutient (Lourens et al., 2008; Ascensão et al., 2001). The aerial parts of the plant contain essential oils, composed mainly of α-pinene, limonene, α-bisabolol, β-caryophyllene, α-humulene, pinocampheol, β-elemene, benzyl benzoate, *allo*-aromadendrene, and *epi*-α-bisabolol, (Ascensão et al., 2001; Chinou et al., 1997a, 1997b; Lourens et al., 2008; Maggio et al., 2016; Roussis et al., 2002; Tsoukatou et al., 1999; Vernin and Poite, 1998). In addition, isomers of caffeoylquinic and dicaffeoyl quinic acids, apigenin glucoside, quercetin, kaempferol, (Lourens et al., 2008), neo-chlorogenic, chlorogenic and crypto-chlorogenic acids, naringenin, tetrahydroxychalcone-glucoside, (Carini et al., 2001), arzanol, 5,7-dihydroxy-3,6,8-trimethoxyflavone, quercetagetin-7-O-glucopyranoside and santinol B are also present (Lavault and Richomme, 2004; Les et al., 2017). A new acylated flavonoid glycoside helichrysoside (3,5-dihydroxy-6,7,8-trimethoxyflavone) was isolated from the golden yellow flower heads of *Helichrysum kraussii* (Candy et al., 1975).

In-silico approaches such as molecular docking is considered as one of the fundamental elements of drug designing and discovery paradigms aimed at elucidating ligand-receptor interaction mechanisms and assisting lead optimization (Azam et al., 2012, 2020). This technique is routinely used to accelerate the recognition and investigation of novel drug candidates (Shushni et al., 2013).

In this study, several experimental techniques were implemented to isolate, characterize and scrutinize anti-inflammatory and analgesic potencies of lanostane triterpenoid glycosides from ethanolic extract of *H. stoechas*. The molecular docking study was employed to ascertain the binding mechanism of isolated compounds HS-02, HS-03, and HS-04 with numerous anti-inflammatory drug targets intended to underscore the structural requirements for intermolecular interactions. Mutagenic potential and LD_{50} values were also estimated through computational methods. Diclofenac, a standard drug, was also included for comparative analysis in the *in-silico* studies.

2. Materials and methods

2.1. Collection and authentication of plant material

We collect 3.5 kg weight of the fresh plant sample from the basin of the Mediterranean Sea, Misurata (latitude-32.377533, longitude-15.092017 and altitude-0.10 m), Libya in March 2015, which was authenticated by Dr. Huda Elgubbi, Department of Botany, College of Science, Misurata University, Misurata, Libya. A voucher specimen no. HC 55/01 has been submitted within the herbarium, Department of Botany, College of Science, Misurata University, Misurata, Libya for the proceedings.

2.2. Extraction and isolation

The aerial parts of plant *H. stoechas* 3.5 kg were shade dried, crudely pulverized, and 500 g powder extracted thoroughly with 95% ethanol using the Soxhlet apparatus. The ethanol extract was then placed on a water bath and dried under reduced pressure to yield 87.9 g of dark brown mass. Numerous components were separated from the extract using a chemical screening method. (Arif & Fareed 2010). For isolation of phytoconstituents, about 80 g of the extract were chromatographed using silica gel (60–120) eluting with solvent mixtures of increasing polarities such as petroleum ether, chloroform, and methanol, were used in various ratios (petroleum ether : chloroform − 9:10, 3:1, 1:1, 1:3 v/v and chloroform: methanol − 99:1, 98:2, 97:3, 24:1, 19:1, 9:1, 3:1, and 1:1, 1:3 v/v) (Ansari et al., 2016). Elution of the column with chloroform gave colorless crystals of HS-02, 102 mg (0.314 % yield). Elution of the column with chloroform: methanol (18:02) mixture yielded colorless crystalline compound HS-03, 115 mg (0.19 % yield) and straw color compound HS-04, 123 mg (0.311% yield).

2.3. Instrumentation, chemicals, and drugs

Melting point apparatus (Perfit), ultraviolet (UV) spectra (Lambda Bio 20 Spectrophotometer Shimadzu-U Singapore) scanned in chloroform, infrared (IR) spectra (Win IR FTS 135 instrument, Biorad, USA), ^1H nuclear magnetic resonance (NMR) 300 MHz and ^{13}C NMR 75 MHz spectra in CD_3OD (Brucker Spectrometer, Brucker, USA), MS (DART dry Helium, JEOL-Accu TOF JMS-T100LC), plethysmometer (UGO Basil, Italy). Carrageenan was procured from Sigma Chemical Co., St. Louis, MO. Standard drugs Indomethacin, Diclofenac, and Tramadol as a gift sample from Ranbaxy labs, New Delhi. The solvents for isolation were acquired from Merck Germany. Silica gel (60–120) mesh, Merck, Germany)

for column chromatography and thin-layer chromatography, silica gel G coated TLC plates (Merck, Germany) was utilized. Spots were visualized by exposure to iodine vapors, UV Lamp

254 nm, and by spraying with anisaldehyde sulphuric acid reagents or with iodine vapors. The percentage yields of the isolated compound were calculated based on dried plant material (500 g) is used for extraction (Hussain et al., 2019).

2.4. Animals

Healthy Wistar albino rats of both sexes weighing between 140 and 160 g were preferred for anti-inflammatory activity and adult Swiss albino mice of every sex (25–30 g) for analgesic activity. They were maintained in clean, sterile, polypropylene cages at room temperature (21 ± 2 °C) in 12 h dark/light control and fed with commercial pellet and water *ad libitum*. After randomization into various groups, the mice were quarantined for a week for environmental and handling acclimatization before the initiation of experiments. The experimental procedure was permitted by Institutional Ethical Committee, Faculty of Pharmacy, Misurata University, Misurata, Libya, and their guidelines were followed for the studies (Phar-01/2015).

2.4.1. Safety profile study

An acute toxicity study was conceded out for the assurance of LD_{50} by carrying out the plan (Annexure 2d) of CPCSEA, OECD guideline No. 423. Swiss albino mice of each sex were alienated into seven groups with six animals in each group. Isolated compounds HS-02, HS-03, and HS-04 from ethanolic extract of *H. stoechas* at various dose levels of 50, 100, and 150 mg/kg were administered orally as a single dose to mice. The animals were observed periodically for the indication of toxicity and death for 24 h and afterward consistently for 14 days (Hussain et al., 2016).

2.4.2. Administration of drugs

The isolated compounds HS-02, HS-03, and HS-04 at doses 05 and 10 mg/kg were administered in all the experimental mod-

Table 1 ^1H and ^{13}C NMR spectral values of Lignoceric acid (HS-02).

Position of proton	Nature of proton	δ_H (ppm)		δ_C (ppm)
		α	β	
C_1	C	–	–	177.21
C_2	CH_2	2.37 (t, J = 7.2)	2.28	33.85
C_3	CH_2	2.06	1.98 (m)	32.15
C_3	CH_2	1.63	1.58 (m)	29.92
C_4	CH_2	1.53	1.47 (m)	29.90
C_5	CH_2	1.31	–	29.88
C_6	CH_2	1.25	1.29 (brs)	29.86
C_7	CH_2	1.25	1.29 (brs)	29.85
C_8	CH_2	1.25	1.29 (brs)	29.84
C_9	CH_2	1.25	1.29 (brs)	29.83
C_{10}	CH_2	1.25	1.29 (brs)	29.81
C_{11}	CH_2	1.25	1.29 (brs)	29.80
C_{12}	CH_2	1.25	1.29 (brs)	29.79
C_{13}	CH_2	1.25	1.29 (brs)	29.78
C_{14}	CH_2	1.25	1.29 (brs)	29.76
C_{15}	CH_2	1.25	1.29 (brs)	29.72
C_{16}	CH_2	1.25	1.29 (brs)	29.69
C_{17}	CH_2	1.25	1.29 (brs)	29.67
C_{18}	CH_2	1.25	1.29 (brs)	29.58
C_{19}	CH_2	1.25	1.29 (brs)	29.30
C_{20}	CH_2	1.25	1.29 (brs)	27.81
C_{21}	CH_2	1.28	1.31	26.27
C_{22}	CH_2	1.28	1.31	24.98
C_{23}	CH_2	1.30	1.34	22.91
C_{24}	CH_3	0.83 (t, J = 6.5)		14.33

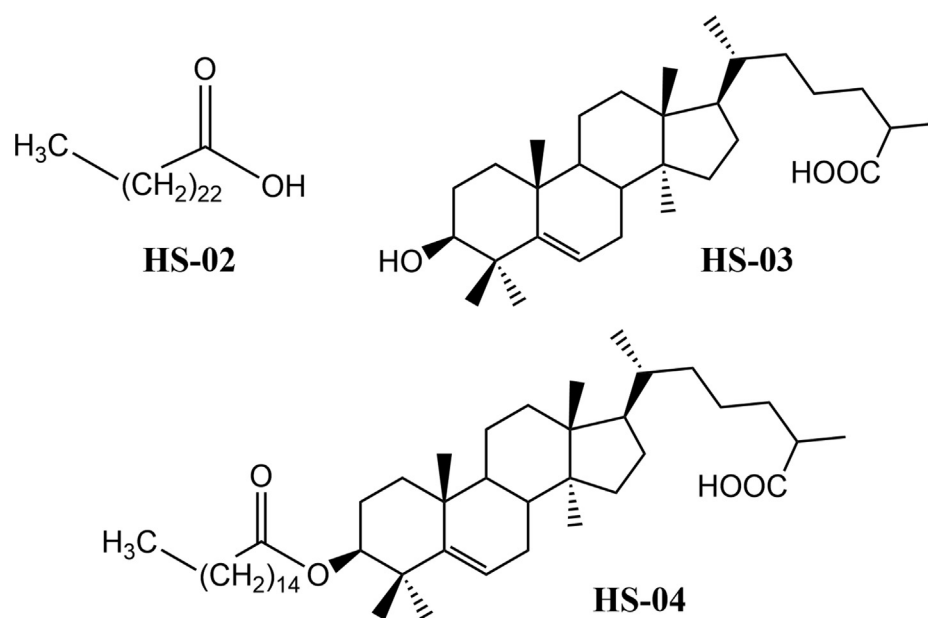Coupling constants in Hz are provided in parentheses.

Fig. 1 Chemical structures of isolated compound lignoceric acid (HS-02), lanost-5- en-3β-ol- 26-oic acid (HS-03). lanost-5-en-26-oic acid-3β-olyl palmitate (HS-04).

Table 2 ^1H and ^{13}C NMR spectral values of Lanost-5- en-3β-ol- 26-oic acid **(HS-03)**.

Position of proton	Nature of proton	δ_H (ppm) α	β	δ_C (ppm)
C_1	CH_2	1.23 (brs)	1.27	34.73
C_2	CH_2	1.38 (brs)	1.45	27.68
C_3	CH	3.22 (dd, J = 5.4)		78.17
C_3	CH	4.65	OH	–
C_4	C	–	–	39.51
C_5	C	–	–	138.81
C_6	CH	5.25 (m)		119.72
C_7	CH_2	2.27	2.31(m)	29.26
C_8	CH	2.14 (d, J = 6.0)		42.05
C_9	CH	2.11		48.28
C_{10}	C	–	–	38.65
C_{11}	CH_2	2.17	2.20	21.08
C_{12}	CH_2	1.98	2.02	23.21
C_{13}	C	–		48.38
C_{14}	C	–		55.96
C_{15}	CH_2	1.87 (brs)	1.90	35.92
C_{16}	CH_2	1.62 (brs)	1.68	48.13
C_{17}	CH	1.81(m)		55.27
C_{18}	CH_3	0.76 (brs)		14.02
C_{19}	CH_3	0.93 (brs)		17.03
C_{20}	CH	2.49 (d, J = 5.7)		30.42
C_{21}	CH_3	0.90 (d, J = 6.1)	–	15.49
C_{22}	CH_2	1.17		35.42
C_{23}	CH_2	1.13	1.08	33.68
C_{24}	CH_2	1.03		31.16
C_{25}	CH	1.54 (d)		29.52
C_{26}	COOH	0.78		176.89
C_{27}	CH_3	0.87 (d, J = 6.3)		22.18
C_{28}	CH_3	0.78 (brs)		20.21
C_{29}	CH_3	0.98 (brs)		28.03
C_{30}	CH_3	1.08 (brs)		14.08

els. Indomethacin 10 mg/kg was utilized as a standard anti-inflammatory drug, Tramadol 0.1 ml (40 mg/kg. s.c) was used as pain inhibiting drug in hot plate technique, and Diclofenac 5 mg/kg was use d as pain inhibiting drug in acetic acid per-

suade writhing in mice. All the test and standard medications were formulated into an emulsion using 0.3% Carboxy Methyl Cellulose (CMC) to obtain the desired dose on a bodyweight basis (mg/kg) of the animal and administered orally utilizing a ball finished taking care of needle. The animals were permitted free admittance to water and food in the wake of dosing (Iqbal et al., 2016).

2.4.3. Carrageenan-induced rat hind paw edema

Acute inflammation was incited by injection of 0.1 ml of 1% freshly prepared suspension of carrageenan in normal saline in the sub-plantar region of the right hind paw of all teams of animals (Mukherjee et al., 1997). At 1, 2, 3, 4, and 5 hr spans the volume of the injected paws was measured using a plethysmometer. The animals were premedicated with vehicle (0.3% CMC p.o.), isolated compounds HS-02, HS-03, and HS-04 at doses 05 and 10 mg/kg, and standard drug indomethacin (10 mg/kg) 1hr before carrageenan challenge (Sachan et al., 2011). The percentage inhibition of inflammation was meant consistent with the subsequent formula: % inhibition = 100 (1-Vt/Vc), Where 'Vc' stands for inflammation volume in control and 'Vt' inflammation volume in the group treated with tested drugs.

2.4.4. Analgesic activity

Analgesic activity of the isolated compounds HS-02, HS-03, and HS-04 was determined by both chemical (acetic acid-induced writhing response) and thermal method (hot plate reaction time).

2.4.4.1. Hot plate test. The pain-relieving (analgesic) test was done by Eddy's hot plate maintained at a temperature of 55 ± 1 °C. The basal response time of all mice towards thermal heat was verified first, then they were medicated with vehicle (0.3% CMC p.o.), isolated compounds HS-02, HS-03, and HS-04 at dose 05 and 10 mg/kg and standard medication Tramadol 0.025 ml (10 mg/kg. s.c). Following an hour of the test and standard medication dosing, the mice in all groups were individually placed to the hot plate maintained at 55 °C. The snapshot of time required in seconds for paw licking or bounc-
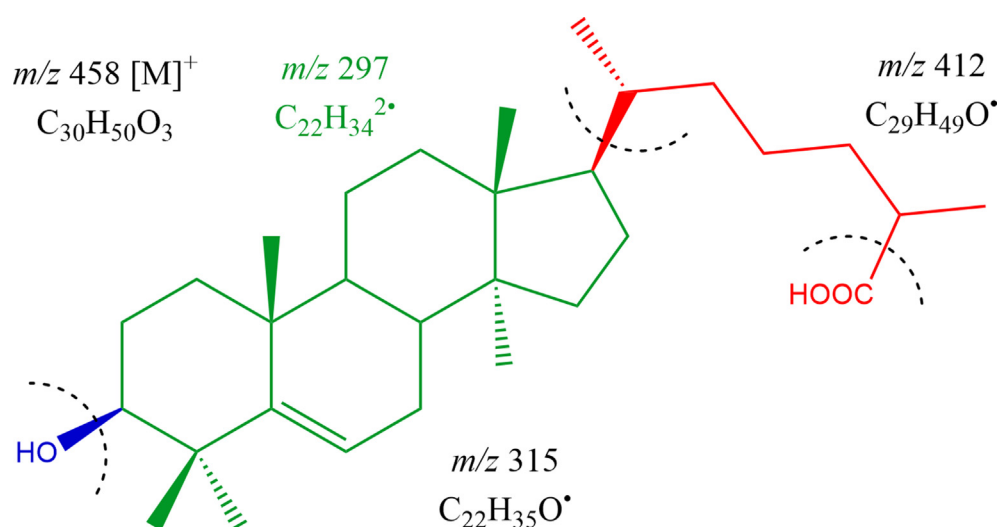

Fig. 2 Mass fragmentation pattern of Lanost-5- en-3β-ol- 26-oic acid (HS-03).

ing was noted as reaction time. A remove phase of 30 s is kept up to dodge the paw's harm. The pain inhibition percentage (PIP) was determined by the accompanying equation (Delporte et al., 2005).

Pain inhibition percentage $(PIP) = ((T_1 - T_0)/T_0) \times 100$

T_1 is post-drug latency and T_0 is pre-drug latency time.

2.4.4.2. Acetic acid-induced writhing test. The animals were pre-medicated with vehicle (0.3% CMC p.o.), HS-02, HS-03, and HS-04 at doses 05 and 10 mg/kg and standard medication diclofenac (5 mg/kg). Acetic acid (1% *v/v*) at the dose of 1 ml/kg body weight was injected intra-peritoneally to all the groups of animals 1hr after the dosing of test and standard drugs. Writhing was recorded by counting the number of writhes following the injection of acetic acid for a time of 30 min. The writhe is signified by abdominal constriction and full extension of the hind limb (Sajad et al., 2009).

2.5. Molecular docking

Chemical structures of isolated compounds HS-02, HS-03, and HS-04 were drawn using the ChemDraw program and converted to their three-dimensional coordinates in Chem3D. Structural coordinates of diclofenac was obtained from PubChem database in sdf format. Each ligand was subjected to energy minimization by the MM2 method and saved in pdb format. The three-dimensional structures of several drug targets associated with inflammatory cascade were retrieved from the Protein Data Bank (http://www.rcsb.org/pdb/home/home.do) and handled in Biovia Discovery Studio Visualizer 2020 program for checking any missing residue/atom and deleting co-crystallized molecules such as cofactors, inhibitors, and water. MGL Tools 1.5.6 was used for assigning Gasteiger charges on ligands and receptor proteins after merging non-polar hydrogens and saved as pdbqt format. The binding site in each receptor was defined according to the co-crystallized inhibitors. A grid box with dimensions of 30, 30, and 30 points in x, y, and z directions was built with a grid spacing of 1 Å. Molecular docking was performed using AutoDock Vina (Trott and Olson) with default parameters, and the exhaustiveness value was set to 12. Each docking involves ten independent runs keeping rigid protein and flexible ligand. Finally, upon successful completion of docking simulation, the best poses of each ligand were screened by inspecting binding energy ($\Delta G_{binding}$, kcal/mol). Molecular interactions of ligand–protein complexes were studied using Biovia Discovery Studio Visualizer 2020 and PyMol 2.4.1 programs.

2.5.1. In silico toxicity

The toxicity of the isolated compounds HS-02, HS-03, and HS-04 was evaluated by T.E.S.T. software, Version 5.1.1, a program developed by the US Environmental Protection Agency (Martin 2016). The robust predictiveness of T.E.S.T. relies on innovative quantitative structure–activity relationship computations for toxicity measurement of synthetic as well as natural compounds based on respective molecular frameworks.

2.6. Statistical analysis

A one-way analysis of variance followed by Dunnett's post-hoc test was performed by using Graph Pad Prism V2.01 (GraphPad Software, Inc., San Diego, California, USA). The data were expressed as the mean ± standard error of the mean and $P < 0.05$ and < 0.01 was considered as statistically substantial.

3. Results and discussion

3.1. Structural revelation

Compound HS-02- Transparent crystals; yield 102 mg (0.314 % mg/g); R_F 0.37 (CH_3OH: $CHCl_3$, 1:3); mp 83–

Table 3 ^{1}H and ^{13}C NMR spectral values of Lanost-5-en-26-oic acid-3β-olylpalmitate **(HS-04)**.

Position of proton	Nature of proton	δ_H (ppm) A	β	δ_C (ppm)
C_1	CH_2	1.27 (*brs*)	1.32	34.10
C_2	CH_2	1.53 (*brs*)	1.57	27.68
C_3	CH	4.19 (*dd, J* = 5.4, 8.7)		79.85
C_3	OH	5.01		–
C_4	C	–	–	43.03
C_5	C	–	–	145.34
C_6	CH	5.35 (*d, J* = 5.0.74)		123.27
C_7	CH_2	2.27	2.31 (*m*)	29.17
C_8	CH	2.34 (*d, J* = 6.0)		40.88
C_9	CH	2.13		50.11
C_{10}	C	–	–	38.24
C_{11}	CH_2	2.17	2.20	23.87
C_{12}	CH_2	1.98	2.02	26.24
C_{13}	C	–		47.39
C_{14}	C	–		56.96
C_{15}	CH_2	1.87 (*brs*)	1.90	35.10
C_{16}	CH_2	1.62 (*brs*)	1.68	39.98
C_{17}	CH	1.81(*m*)		54.50
C_{18}	CH_3	0.85 (*brs*)		16.18
C_{19}	CH_3	0.94 (*brs*)		19.62
C_{20}	CH	2.49 (*d, J* = 5.7)		28.91
C_{21}	CH_3	0.87 (*d, J* = 6.3)		17.75
C_{22}	CH_2	1.17	1.12	34.15
C_{23}	CH_2	1.13	1.08	33.21
C_{24}	CH_2	1.03	0.98	31.75
C_{25}	CH	1.54 (*d*)		28.29
C_{26}	COOH	0.78		177.63
C_{27}	CH_3	0.90 (*d, J* = 6.2)		24.27
C_{28}	CH_3	0.95 (*d, J* = 7.8)		21.73
C_{29}	CH_3	0.97 (*brs*)		29.91
C_{30}	CH_3	1.09 (*brs*)		16.47
$C_{1'}$	C	–		166.03
$C_{2'}$	CH_2	2.32 (*t, J* = 7.2)		33.72
$C_{3'}$	CH_2	2.30 (*m*)		33.21
$C_{4'}$	CH_2	2.28 (*m*)		30.90
$C_{5'}$	CH_2	2.28 (*m*)		30.88
$C_{6'}$	CH_2	2.26 (*m*)		30.88
$C_{7'}$	CH_2	2.24 (*m*)		30.90
$C_{8'}$	CH_2	2.18 (*m*)		30.90
$C_{9'}$	CH_2	2.16 (*m*)		30.75
$C_{10'}$	CH_2	2.14 (*m*)		30.61
$C_{11'}$	CH_2	2.11 (*m*)		30.36
$C_{12'}$	CH_2	1.98 (*brs*)		26.24
$C_{13'}$	CH_2	1.48 (*brs*)		25.47
$C_{14'}$	CH_2	1.32 (*brs*)		24.14
$C_{15'}$	CH_2	1.22 (*brs*)		22.68
$C_{16'}$	CH_3	0.84 (*t, J* = 6.1)		14.99

84 °C; UV–visible λ_{max} (CH$_3$OH): 283 nm; IR ν_{max} (KBr): 3409, 2923, 2856, 1321, 1176, 1148, 1037, 1003, 889, 724 cm^{-1}; ^{1}H NMR (300 Hz, CH$_3$OD);^{13}C NMR (75 Hz, CH$_3$OD) [Data: Table 1]; MS DART m/z (relative intensity) : 368 [M$^+$] (C$_{24}$H$_{48}$O$_2$) (2.8). Compound HS-03 (lignoceric acid) is saturated fatty acid, found as transparent crystals using CHCl$_3$ and CH$_3$OH (9:1) as eluent. Its carboxylic group was confirmed by sodium bicarbonate test: Exhibited effervescence. IR spectroscopy confirmed the presence of OH (3409 cm^{-1}), COOH (1690 cm^{-1}), and aliphatic sequence (724 cm^{-1}). Fragmentation pattern of HS-02 showed parent ion peak on m/z 368; this confirms the presence of C$_{24}$ fatty acid, C$_{24}$H$_{48}$O$_2$. Proton NMR spectrum of HS-02 exhibited a 2H triplet at δ_H 2.37 (J: 7.2 Hz) to confirm the existence of H-2 vinylic protons. Three two-proton multiplets at 2.06, 1.63, and 1.53 and one six proton multiplets at 1.31. A thirty-proton broad singlet at 1.25 were credited to methylene H's contiguous to the carboxylic group. A 3H triplet at δ_H 0.80 (J: 6.5 Hz), integrated 3H's to display the finale (C-24)1° methyl group. ^{13}C NMR spectra of HS-02 demonstrated the C-1 (δ177.21) as carboxylic carbon and C-24 (14.33) methyl carbons. The methylene carbons echoed in the array of δ_H 33.85 to 22.91. The spectral data concluded that compound HS-02 be long-chain saturated fatty acid lignoceric acid (n-tetracosanoic acid) (Fig. 1- HS-02).

Compound HS-03- Lanost-5-en-3α-ol- 26-oic acid, acquired as transparent crystals using CHCl$_3$ and CH$_3$OH (18:02) as eluents, yield 115 mg (0.19 % w/w); R$_F$ 0.49 (CHCl$_3$: Pet ether, 7.5:2.5); mp 90–92 °C; UV–visible λ_{max} (CH$_3$OH): 290 nm; IR ν_{max} (KBr): 3215, 2923, 2856, 1690, 1635, 1461, 1383, 1277, 1193, 1037, 1003, 953 cm^{-1}; ^{1}H NMR (300 Hz, CH$_3$OD) and ^{13}C NMR (75 Hz, CH$_3$OD) [Data: Table 2]; MS DART m/z (relative intensity) : 458 [M]$^+$(C$_{30}$H$_{50}$O$_3$) (5.2), 440 (100), 412 (10.1), 315 (21.2), 297 (41.3) (Fig. 2). It's confirmatory tests for terpenoids and IR absorption bands for OH (3215 cm^{-1}), COOH (1690 cm^{-1}), unsaturation (1635 cm^{-1}), and aliphatic sequence (953 cm^{-1}). Fragmentation pattern indicated the molecular ion peak of HS-03 at m/z 458; this reinforced the molecular formula of triterpenic moiety C$_{30}$H$_{50}$O$_3$. It may be due to the loss of CO$_2$ molecule during the ionization of the compound in position C-26 the molecular ions found in the mass spectra were corresponding to the mass

peak at m/z 412. The compound is fragmented into two parts between C11 and C12 and between C8 and C14. These fragments have m/z 191 and 248 with molecular formula C$_{14}$H$_{22}$ and C$_{18}$H$_{32}$ respectively. ^{1}H NMR spectra of HS-03 exhibited ^{1}H multiplet at δ_H 5.25 ppm (C-6) and 1H double doublet's at δ_H 3.22 (J: 4.5, 5.4 Hz) endorsed vinylic H-6 and oxygenated methine H-3α protons, correspondingly. Two 3H doublet at δ_H 0.90 (J = 6.1 Hz) with 0.87 (J = 6.3 Hz) credited as methyl C-21 and C-27, correspondingly. The five three-proton broad singlets at δ_H 1.08, 0.98, 0.93, 0.78, and 0.76 ascribed tertiary C-30, C-29, C-19, C-28, and C-18 methyl protons, and all methyl functionalities were attached to the saturated carbons. The ^{13}C NMR spectrum of HS-03 displayed signals for vinylic carbons at δ_C 138.81 (C-5) and 119.71 (C-6), carboxylic carbons at δ_C 176.89 (C-26), oxygenated methine carbon δ_C 78.26 (C-3) and the other carbon appears in the range of δ_C 55.06 to 14.03. The ^{1}H and ^{13}C NMR spectral data of the lanostene unit were compared with related triterpenoids (Arif et al., 2013; Hussain et al., 2020b). Based on these results the structure of HS-03 has been formulated as Lanost-5- en-3α-ol- 26-oic acid (Fig. 1-HS-03). This is a new triterpene phytoconstituents of *H. stoechas*.

Compound HS-04- Lanost-5-en-26-oic acid-3β-olyl palmitate-was acquired as straw colour crystals using CHCl$_3$ and CH$_3$OH (18:2) as eluants; 123 mg (0.311% yield); R$_F$ 0.53 (CH$_3$OH: CHCl$_3$, 9:1); mp 100–105 °C; UV–visible λ_{max} (CH$_3$-OH): 278 nm; IR ν_{max} (KBr): 2956, 2856, 1725, 1690, 1635, 1461, 1388, 1262, 1061, 953, 730 cm^{-1}; ^{1}H NMR (300 Hz, CH$_3$OD) and ^{13}C NMR (75 Hz, CH$_3$OD) [Data: Table 3]; MS DART m/z (relative intensity) : 696 [M]$^+$ (C$_{46}$H$_{80}$O$_4$) (2.2), 457 (21.6), 440 (100), 256 (10.4), 239 (8.6). It displayed confirmatory tests for glycosides and IR absorption bands for COOR (1725 cm^{-1}), COOH (1690 cm^{-1}), unsaturation (1635 cm^{-1}), and aliphatic sequence (730 cm^{-1}). Mass spectra demonstrated the molecular ion peak of HS-04 at m/z 696 to confirm the triterpene ester moiety C$_{46}$H$_{80}$O$_4$ (Fig. 3). ^{1}H NMR spectra of HS-04 exhibited a 1 H doublet at δ_H 5.35 (J = 5.7 Hz), 2H double doublet at δ_H 4.19 (J = 5.4, 8.7 Hz) and two 3H proton doublet at δ_H 0.90 (J = 6.2 Hz) and δ_H 0.87(J = 6.3 Hz) endorsed as vinylic H-6, methyl C-27, and C-21, respectively. A 2H triplet's appeared at δ_H
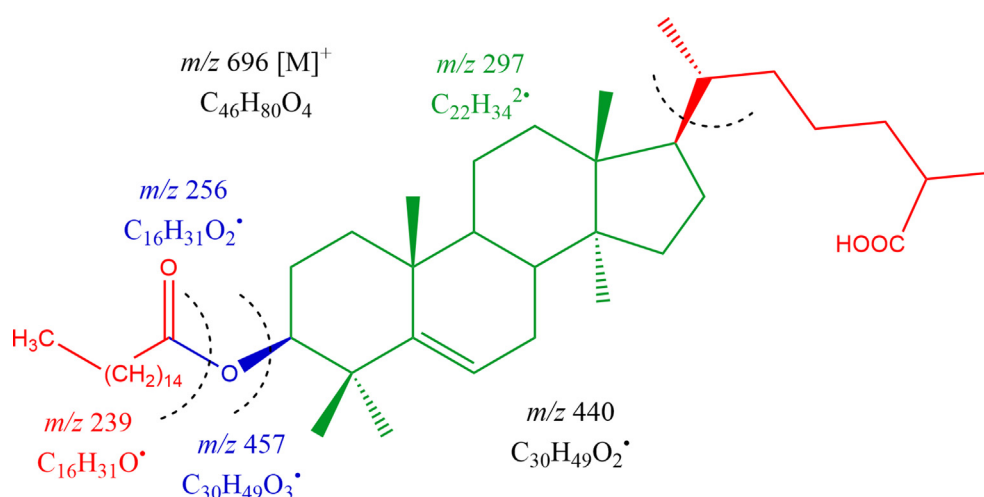

Fig. 3   Mass fragmentation pattern of Lanost-5-en-26-oic acid-3β-olyl palmitate (HS-04).

2.32 (J = 7.2 Hz), one three-proton triplet at δ_H 0.84 (J = 6.1 Hz), and a two proton multiplet's ascribed as methene (C-2′) (C-7) and methyl (C-16′) respectively. The six 3H broad singlet's seemed at δ_H 1.09, 0.97, 0.94, 0.82, 0.80 and 0.77, ascribed as methyl C-30, C-29, C-19, C-27, C-28 and C-18, respectively. The ester Hs appear in the array of δ_H 2.12 to 1.28. ^{13}C NMR spectra of HS-04 exhibited vinylic carbons at δ_C 145.34 (C-5) and 123.27(C-6), COOH carbons at δ_C 177.63 (C-26), oxygenated methine carbon δ_C 79.85 (C-3) and the other carbon appears in the range of δ_C 56.89 to 16.47. The ester carbon appears at δ_C 166.03 (C-1′) and other aliphatic carbon ranges in δ_C 33.72 to 14.99. ^{1}H along with ^{13}C NMR spectral features of the lanostene unit exhibited similarity with related triterpenoids (Hussain et al, 2020a). The struc-tural features of HS-04 confirmed it to be Lanost-5-en-26-oic acid-3β-olylpalamitate (Fig. 1- HS-04). This is a new triter-penoid ester of palmitic acid of *H. stoechas*

3.2. Safety profile study

It was seen that the dosing of isolated compounds HS-02, HS-03, and HS-04 up to 150 mg/kg orally to the mice didn't incite drug-related harmfulness (toxicity) and mortality. The mice endured the drug well and showed normal behavior up to 150 mg/kg orally. All animals were vigilant with normal spruce, touch, and pain response, and there was no indication of accommodation and vocalization.
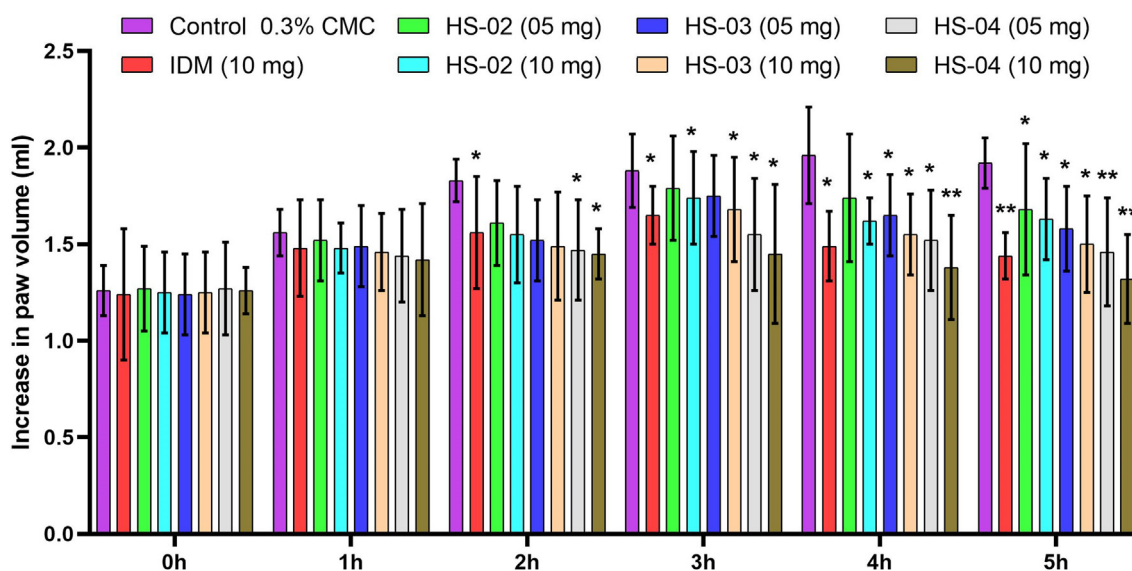

Fig. 4 Effect of of isolated compounds **HS-02**, **HS-03** and **HS-04** and Indomethacin (IDM) on carrageenan induced rat paw edema. Each value is expressed in Mean ± S.E.M. one way ANOVA followed by Dunnett's test. P: *$p < 0.05$ and **$p < 0.01$ compare to respective control group.
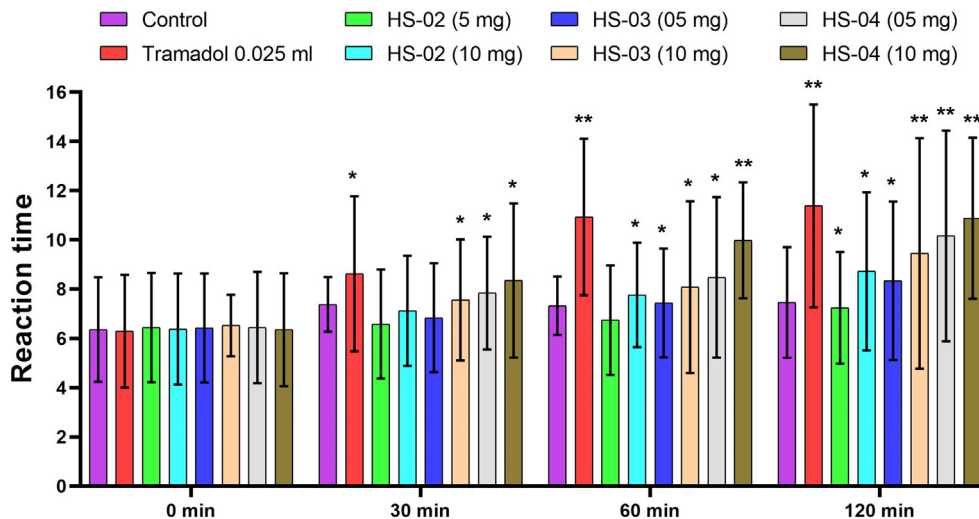

Fig. 5 Effect of isolated compounds **HS-02**, **HS-03**, **HS-04** and Tramadol (Standard) on reaction time of mice exposed to hot plate. Each value is expressed in Mean ± S.E.M. one way ANOVA followed by Dunnett's test. P: *$p < 0.05$ and **$p < 0.01$ compare to respective control group.
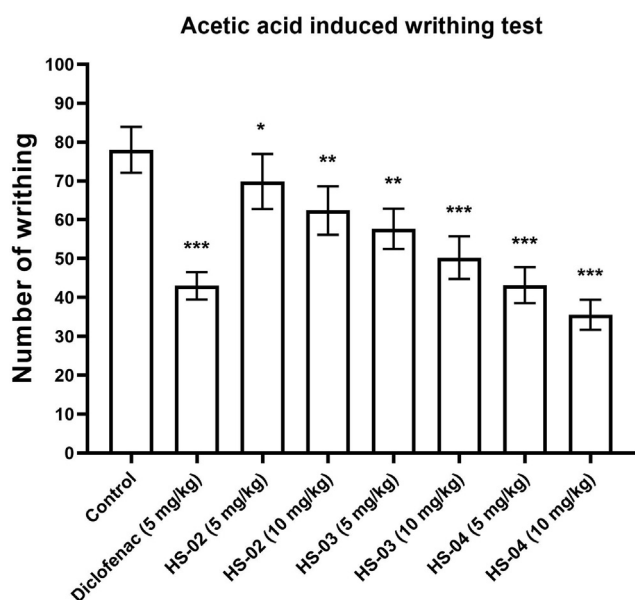
Fig. 6 Effect of isolated compounds HS-02, HS-03, HS-04 and Diclofenac (Standard) on acetic acid induced writhing in mice. Each value is expressed in Mean ± S.E.M. one way ANOVA followed by Dunnett's test. P: *p < 0.05, **p < 0.01 and ***p < 0.001compare to respective control group.

3.3. Carrageenan induced rat paw edema

Anti-inflammatory effect of isolated compounds HS-02, HS-03, and HS-04 at a dose (05 & 10 mg/kg) and Indomethacin at a dose (10 mg/kg) on carrageenan disturbed rat paw is displayed in (Fig. 4). The anti-inflammatory effects of all tested drugs were seen from 60 min. after carrageenan challenge. Paw edema in rats accomplished its highest at 4 hrs following carrageenan challenge and animals treated with Indomethacin

showed a significant (P < 0.05) decrease in paw volume of rats from 2 hr. Treatment with Indomethacin and HS-04 at (10 mg/kg) showed a significant reduction (P < 0.05) of paw volume in rats incited by carrageenan. The impact of HS-04 at portion 10 mg/kg was discovered favored in lessening the swollen paw volume than a higher portion of Indomethacin (10 mg/kg). Aggravation is associated with a ton of pathophysiologies of various clinical conditions like joint inflammation, malignant growth, gout, and vascular sicknesses. A lot of therapeutic plants are utilized in the scope of conventional clinical frameworks for the help of caution indication of torment and irritation. In this investigation, the lignoceric acid (HS-02), lanost-5-en-3β-ol- 26-oic acid (HS-03), and lanost-5-en-26-oic acid-3β-olyl palmitate (HS-04) isolated from *H*. *stoechas* extract showed calming pain-relieving action at dose 05 and 10 mg/kg. Carrageenan is gone about as a phlogistic factor and increased the prostaglandins and bradykinins combination at different periods (He et al., 2005). All tested drugs showed a decrease in paw edema volume from 1hr to 5hr and prolong its anti-inflammatory effect after the 3hr. This investigation unmistakably shows that the impact of all tested drugs may cooperate with the prostaglandins spurt. Curiously both dose levels of HS-04 exhibited a similar pattern in reducing carrageenan-induced paw edema from 1hr to 5hr. Carrageenan-induced inflammation is caused by the commencement of prostaglandins, platelet-activating factors (PAF), and other inflammatory mediators. The primary stage (0-1hr) is supported by the arrival of histamine, 5-HT, and kinin, though the subsequent stage (3–5 hr) is associated with the release of prostaglandin and bradykinin. Even though the calming response found in 10 mg/kg was superior to the 05 mg/kg. This result straightforwardly correlated with the results observed in carrageenan-induced paw edema where both doses of isolated compounds significantly alter the carrageenan initiated prostaglandins intervened inflammatory response (Mukherjee et al., 1997).
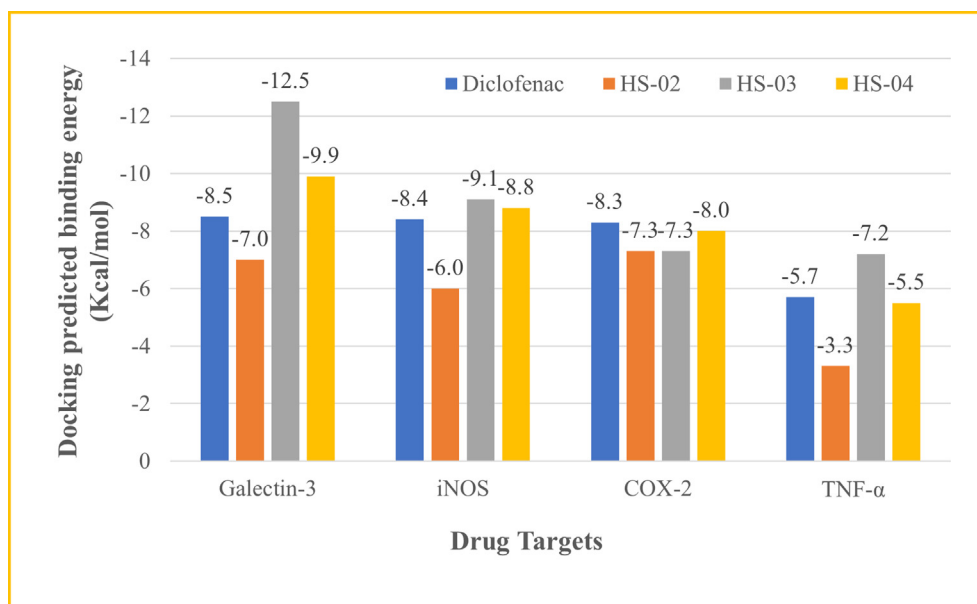

Fig. 7 Docking predicted binding energy of isolated compounds and standard drug, diclofenac, plotted against protein targets such as galectin-3, iNOS, COX-2, and TNF-α.

3.3.1. Hot plate test

HS-03 and HS-04 at dose 10 mg/kg and Tramadol significantly (P < 0.01) augmented the response time of animals towards the thermal source with various periods (Fig. 5). In hot plate test of isolated compounds HS-02, HS-03 and HS-04 at dose (10 mg/kg p.o.) and Tramadol (10 mg/kg. s.c) displayed a pain inhibition percentage (PIP) of 36.67%, 44.93%, 72.97% and 79.21%.

3.3.2. Acetic acid-induced writing methods

The analgesic activity of HS-02, HS-03, and HS-04 at doses 05 and 10 mg/kg and Diclofenac (5 mg/kg) was assessed by acetic acid-induced writhing test in mice. Both HS-04 and Diclofenac significantly (P < 0.001) lowered the quantity of abdominal constriction and draw out of hind limbs provoked by the injection of acetic acid (Fig. 6). The percentage of lowering the quantity of abdominal constriction in HS-02, HS-03, and HS-04 at 10 mg/kg was 48.71%, 65.38%, and 84.61%, whereas standard drug Diclofenac (5 mg/kg) showed 71.79%. The abdominal constrictions observed after the challenge of acetic acid are associated with the sensitization of nociceptive receptors to prostaglandins. So subsequently conceivable outcomes of the concentrates apply their pain-relieving impacts maybe by hindering the amalgamation of prostaglandins.
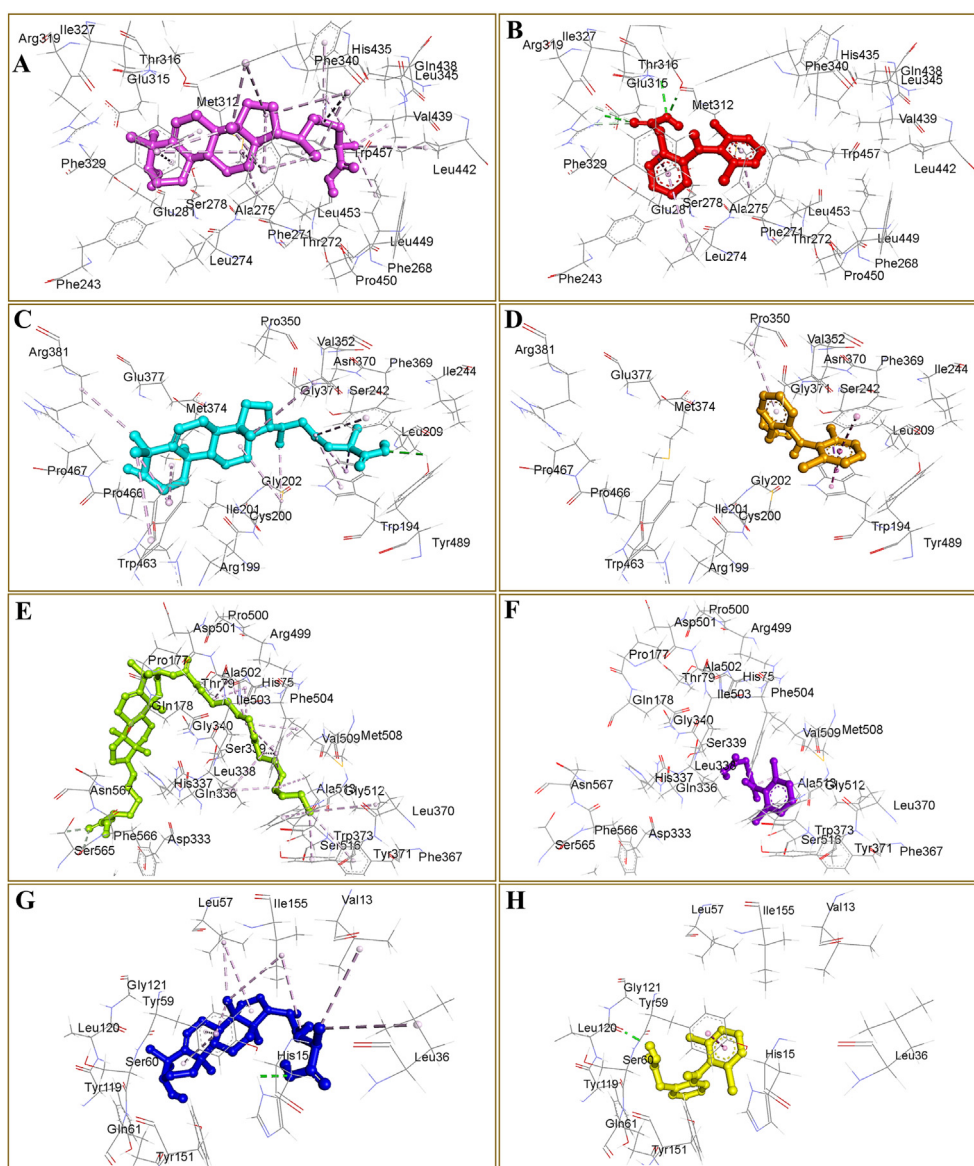

Fig. 8 Three-dimensional conformations of the docked compound HS-03 (A, C, E and G) and diclofenac (B, D, F and H) against galectin-3 (A-B), iNOS (C-D), and TNF-α (E-F). Docked compounds HS-04 and diclofenac in complex with COX-2 are presented in panels G and H, respectively. All docked compounds are shown as ball and stick style whereas binding site residues are represented as lines. Non-bond interactions are displayed as broken green (hydrogen bonds) and purple (hydrophobic) lines.

3.4. Molecular docking

All the isolated compounds HS-02, HS-03, and HS-04 were docked with numerous receptors known to be associated with inflammatory pathways, namely cyclooxygenase-2 (PDB id: 3LN1), tumor necrosis factor-α (PDB id: 2AZ5; He et al., 2005), inducible nitric oxide synthase (iNOS) (PDB id: 4NOS; Fischmann et al., 1999) and galectin-3 (PDB id: 1P8D; Williams et al., 2003). The docking protocol implemented in AutoDock Vina was validated by redocking all co-crystallized ligands with respective proteins. The docked poses were compared with crystal conformation of each ligand exhibiting root-mean-square deviation (RMSD) of ≤ 2.0 Å which confirms the reliability of the opted docking methodology (Ahmed et al., 2012; Azam et al., 2019; 2015).

According to the docking results presented in Fig. 7, HS-03 showed the highest docking scores of −12.50, −9.10, and −7.20 kcal/mol against galectin-3, iNOS, and TNF-α receptors, respectively. However, HS-04 was observed as most active against the COX-2 enzyme displaying −8.0 kcal/mol docking predicted binding energy. Interestingly, HS-02 was noted as the least active molecule against all docked targets confirming that aliphatic carboxylic acid appended with a long unbranched carbon chain failed to afford favorable occupation in the binding sites. However, both HS-03 and HS-04 constitute lanostanol-based steroidal nucleus, suitable for interacting with most of the receptors (Fig. 8). Standard drug diclofenac was also included in the docking study for comparative analysis, which exhibited docking score of −8.50, −8.40, −8.30, and −5.70 kcal/mol against galectin-3, iNOS, COX-2, and TNF-α receptors, respectively. The binding interactions of diclofenac were almost similar to other docked compounds,

following the native co-crystallized ligands of respective proteins. Intermolecular interactions constituting both hydrophilic and hydrophobic contacts of all docked compounds are presented in Table 4. These outcomes are supposed to assist lead optimization and drug development for the treatment of inflammatory disorders.

3.4.1. In-silico toxicity prediction

The unique molecular framework of chemical compounds is usually exploited for the generation of advanced mathematical models for quantitative structure–activity relationship (QSAR) studies aimed at prediction of biological activity as well as toxicity. In particular, the toxicity potential of several compounds was successfully predicted by implementing these models (Claeys et al., 2013; Li et al., 2020; Sripriya et al., 2019). The acute toxicity of isolated compounds HS-02, HS-03, and HS-04 was assessed by using the TEST program which predicts mutagenicity and oral lethal dose for 50% of test rats (LD_{50}). This program uses three diverse methods for prediction, namely, consensus, hierarchical clustering, and nearest neighbor. The computed values of LD_{50} and mutagenicity have been tabulated in Table 5. All tested compounds HS-02, HS-03 and HS-04 exhibited negative mutagenicity scores. However, a positive mutagenicity score was recorded for diclofenac according to consensus and nearest neighbor methods whereas hierarchical clustering method indicated negative result by the TEST program. Several bioassay data show that diclofenac lacks toxicity risks such as carcinogenicity in rodents. However, additional research has recently been published that demonstrates that diclofenac has a genotoxic potential in newer or modified in vitro test systems (Hartmann et al., 2021) (see Table 5).

Table 4 Intermolecular interactions observed after docking of isolated compounds HS-02, HS-03 and HS-04 with probable drug targets.

Target; PDB code	H-bonds				Hydrophobic			
	HS-02	HS-03	HS-04	Diclofenac	HS-02	HS-03	HS-04	Diclofenac
Galectin-3; 1P8D	Met312	–	–	Thr316, Arg319	Phe243, Phe271, Leu274, Ala275, Met312, Leu313, Phe329, Ile353, Phe340, Leu345	Phe271, Ala275, Phe329, Phe340, Leu345, Phe349, His435, Val439, Leu442, Leu449, Trp457	Leu236, Phe271, Ala275, Ile282, Phe285, Ile311, Arg319, Phe329, Phe340, Leu345, Phe349, Ile374, His435, Val439, Leu442, Leu449, Trp457	Leu274, Ala275, Met312, Phe329
Inducible Nitric Oxide Synthase; 4NOS	Arg199, Tyr490, Tyr491	Tyr489	Gly202, Gln492	Trp372	Trp194, Ala197, Pro198, Arg199, Cys200, Pro350, Phe369	Trp194, Cys200, Leu209, Val352, Phe369, Met374, Arg381, Trp463	Leu125, Trp194, Ala197, Pro198, Arg199, Cys200, Pro350, Val352, Phe369, Trp463, Phe488, Tyr489, Tyr491	Trp194, Pro350, Phe369
TNF-α; 2AZ5	Ser60	His15	Gly121	Leu120	Leu57, Tyr59	Val13, Leu36, Leu57, Tyr59, Ile155	Leu57, Tyr59, Tyr119	Tyr59
COX-2; 3LN1	Leu338	Thr79, Asp333	Ser565	–	Val102, Val335, Leu338, Leu345, Leu370, Tyr371, Trp373, Phe504, Met508, Val509, Ala513	His80, His342, Pro500	His75, Leu338, Trp373, Ala502, Phe504, Val509	Val335, Ala513, Leu517

Table 5 Predicted toxicity results of isolated compounds by TEST program.

Prediction methods	Toxicity parameters	Toxicity results			
		HS-02	HS-03	HS-04	Diclofenac
Consensus method	Oral rat LD_{50} mg/kg	20861.82	477.13	326.66	244.02
	Mutagenicity value	0.00	0.30	0.18	0.53
	Mutagenicity result	Negative	Negative	Negative	Positive
Hierarchical clustering method	Oral rat LD_{50} mg/kg	13878.45	104.79	146.60	228.56
	Mutagenicity value	0.00	0.26	0.03	0.40
	Mutagenicity result	Negative	Negative	Negative	Negative
Nearest neighbor method	Oral rat LD_{50} mg/kg	31359.08	2172.48	727.88	260.53
	Mutagenicity value	0.00	0.33	0.33	0.67
	Mutagenicity result	Negative	Negative	Negative	Positive

4. Conclusion

The present study suggested that HS-03 and HS-04 at 10 mg/kg showed significant anti-inflammatory, analgesic activity. Carrageenan incited edema is the principle pull for the actuation of prostaglandins, platelet initiating factors (PAF), and other fiery mediators. In conclusion Lanost-5- en-3β-ol- 26-oic acid (HS-03) and Lanost-5-en-26-oic acid-3β-olyl palmitate (HS-04) isolated from *H. stoechas* extract showed protection against inflammation; pain and cytokine-like pro-inflammatory mediators release might be beneficial in the treatment of endotoxin associated systemic inflammation. To our knowledge, the current study has been conducted for the first time concerning the occurrence of lanostane triterpenoid in ethanolic extract of *H. stoechas*. The study also affirms that these potent isolated compounds may be a valuable marker for the *Helichrysum* genus. These outcomes are relied upon to be essential in lead to augment and fostering the potent molecules HS-03 and HS-04 for the treatment of inflammation-mediated diseases.

Declaration of Competing Interest

The authors declare that they have no known competing financial interests or personal relationships that could have appeared to influence the work reported in this paper.

Acknowledgements

Compliance with ethical standards

Ethical statement: The experimental protocols were approved by the Institutional Ethical Committee of Faculty of Pharmacy, Misurata University, Misurata, Libya, and their guidelines were followed for the studies (Phar-01/2015).

Author Contributions

Md. Sarfaraj Hussain designed and supervised the entire work and wrote the chemistry part of the manuscript, Faizul Azam performed and wrote the results of the docking study, Hanan Ahmed Eldarrat isolated and identified lignoceric acid, lanost-5- en-3β-ol- 26-oic acid and lanost-5-en-26-oic acid-3β-olyl palmitate, Muhammad Arif & Mohammed Ali interpreted the spectroscopic data and revised the manuscript, Mohd. Zaheen Hassan & Anzarul Haque provided the carrageenan and helped in the anti-inflammatory, analgesic study, Irfan Ahmad, Gaffar Zaman, Nadiyah M. Alabdallah, and Mohd. Saeed designed and revised the submitted manuscript.

Appendix A. Supplementary material

Supplementary data to this article can be found online at https://doi.org/10.1016/j.arabjc.2022.103818.

References

Ahmed, M.A., Azam, F., Rghigh, A.M., Gbaj, A., Petrini, A.E., 2012. 'Structure-based design, synthesis, molecular docking, and biological activities of 2-(3-benzoylphenyl) propanoic acid derivatives as dual mechanism drugs. J. Pharm. Bioallied. Sci. 4 (1), 43–50.

Ansari, V.A., Arif, M., Siddiqui, H.H., Dixit, R.K., 2016. Antiplatelet activity and isolation of triterpenoid glycoside from ethanolic extract of *Nepeta hindostan*. Ori. Pharm & Expt. Med. 16 (4), 333–337.

Arif, M., Fareed, S., 2010. Pharmacognostic investigation and authentication of potentially utilized fruit *Spondias mangifera* (Willd). Int. J. Curr. Pharmaceut. Clin. Res. 2 (1), 31–35.

Arif, M., Fareed, S., Hussain, T., 2013. Adaptogenic activity of lanostane triterpenoid isolated from *Carissa carandas* fruit against physically and chemically challenged experimental mice. Pharmacog. J. 5, 216–220.

Ascensão, L., Da Silva, J.A.T., Barroso, J.G., Figueiredo, A.C., Pedro, L.G., 2001. Glandular trichomes and essential oils of *Helichrysum stoechas*. Israel J. Plant Sci. 49, 115–122.

Azam, F., Taban, I.M., Eida, E.E.M., Iqbald, M., Alam, O., Khan, S., Mahmood, D., Anwar, M.J., Khalilullah, H., Khan, M.U., 2020. An *In-silico* analysis of ivermectin interaction with potential SARS-CoV-2 targets and host nuclear importin α. J. Biomol. Struc. Dyn. https://doi.org/10.1080/07391102.2020.1841028.

Azam, F., Abodabos, H.S., Taban, I.M., Rfieda, A.R., Mahmood, D., Anwar, M.J., Khan, S., Sizochenko, N., Poli, G., Tuccinardi, T., Ali, H.I., 2019. Rutin as promising drug for the treatment of Parkinson's disease: an assessment of MAO-B inhibitory potential by docking, molecular dynamics, and DFT studies. Mol. Simul. 45 (18), 1563–1571.

Azam, F., Mohamed, N., Alhussen, F., 2015. 'Molecular interaction studies of green tea catechins as multitarget drug candidates for the treatment of Parkinson's disease: computational and structural insights. Network. 26 (3–4), 97–115.

Azam, F., Prasad, M.V., Thangavel, N., Shrivastava, A.K., Mohan, G., 2012. 'Structure-based design, synthesis and molecular modeling studies of thiazolyl urea derivatives as novel anti-parkinsonian agents. Med. Chem. 8 (6), 1057–1068.

Candy, H.A., Laing, M., Weeks, C.M., Kruger, G.J., 1975. The crystal and molecular structure of helichrysoside, a new acylated flavonoid glycoside from Helichrysum kraussii. Tetrahedron Lett. 16 (14), 1211–1214.

Carini, M., Aldini, G., Furlanetto, S., Stefani, R., Facino, R.F., 2001. LC coupled to ion-trap MS for the rapid screening and detection of polyphenol antioxidants from Helichrysum stoechas. J. Pharm. Biomed. Anal. 24 (3), 517–526.

Chinou, I.B., Roussis, V., Perdetzoglou, D., Loukis, A., 1997a. Chemical and biological studies on four Helichrysum species of Greek origin. In: Franz, C.h., Máthé, Á., Buchbauer, G. (Eds.), Essential Oils: Basic and Applied Research. Allured Publishing Corp, Carol Stream, IL, pp. 45–48.

Chinou, I.B., Roussis, V., Perdetzoglou, D., Tzakou, O., Loukis, A., 1997b. Chemical and antibacterial studies of two Helichrysum species of Greek origin. Planta Med. 63 (2), 181–183.

Claeys, L., Iaccino, F., Janssen, C.R., Van Sprang, P., Verdonck, F., 2013. Development and validation of a quantitative structure-activity relationship for chronic narcosis to fish. Environ. Toxicol. Chem. 32 (10), 2217–2225.

Delporte, C., Backhouse, N., Erazo, S., 2005. Analgesic-anti-inflammatory properties of Proustia pyrifolia. J. Ethnopharmacol. 99, 119–124.

Fischmann, T.O., Hruza, A., Niu, X.D., Fossetta, J.D., Lunn, C.A., Dolphin, E., Prongay, A.J., Reichert, P., Lundell, D.J., Narula, S. K., Weber, P.C., 1999. Structural characterization of nitric oxide synthase isoforms reveals striking active-site conservation. Nat. Struct. Biol. 6 (3), 233–242.

Giuliani, C., Lazzaro, L., Calamassi, R., Calamai, L., Romoli, R., Fico, G., Foggi, B., Lippi, M.M., 2016. A volatolomic approach for studying plant variability: the case of selected Helichrysum species (Asteraceae). Phytochem. 130, 128–143.

Hartmann, A., Erkman, L., Maremanda, N., Elhajouji, A., Martus, H.-J., 2021. Comprehensive review of genotoxicity data for diclofenac. Mutat. Res. Genet. Toxicol. Environ. Mutagen. 866,. https://doi.org/10.1016/j.mrgentox.2021.503347 503347.

He, M.M., Smith, A.S., Oslob, J.D., Flanagan, W.M., Braisted, A.C., Whitty, A., Cancilla, M.T., Wang, J., Lugovskoy, A.A., Yoburn, J. C., Fung, A.D., Farrington, G., Eldredge, J.K., Day, E.S., Cruz, L. A., Cachero, T.G., Miller, S.K., Friedman, J.E., Choong, I.C., Cunningham, B.C., 2005. Small-molecule inhibition of TNF-alpha. Science 310 (5750), 1022–1025.

Hussain, M.S., Ali, M., Mir, S.R., Sultana, S., 2020a. Chemical constituents from the leaves of Carya illinoinensis, aerial parts of Helichrysum stoechas and hulls of Oryza sativa. Euro. J. Pharm. Med. Res. 7 (7), 723–731.

Hussain, M.S., Nazeer Ahamed, K.F.H., Ravichandiran, V., Ansari, M.Z.H., 2009. Free radical scavenging capacity of natural terpenes from Hygrophila auriculata (Schum) Heine. Asian J. Trad. Med. 4 (5), 179–187.

Hussain, M.S., Azam, F., Nazeer Ahamed, K.F.H., Ravichandiran, V., Alkskas, I., 2016. Anti-endotoxin effects of terpenoids fraction from Hygrophila auriculata in lipopolysaccharide-induced septic shock in rats. Pharm. Bio. 54 (4), 628–636.

Hussain, M.S., Ismail, H., Fareed, S., Ali, M., 2019. New aliphatic ester constituents from Hygrophila auriculata (K.Schum) Heine from the basin area of Koshi River. Ori. Pharm and Exp. Med. 19 (3), 251–258.

Hussain, M.S., Eldarrat, H.A., Alkskas, I., Mayoof, J.A., Dammona, J.M., Ismail, H., Ali, M., Arif, M., Haque, A., 2020b. Anti-inflammatory, analgesic activity and molecular docking studies of Lanostanoic acid 3-O-α-D-glycopyranoside isolated from Helichrysum stoechus against chemically challenged experimental animal. Arabian J. Chem. 13 (12), 9196–9206.

Iqbal, S.S., Mujahid, M., Kashif, S.M., Khalid, M., Badruddeen, Arif, M., Bagga, P., Akhtar, J., Rahman, M.A., 2016. Protection of hepatotoxicity using Spondias pinnata by prevention of ethanol induced oxidative stress, DNA-damage and altered biochemical markers in Wistar rat. Integr. Med. Res. 5, 267–275.

Lavault, M., Richomme, P., 2004. Constituents of Helichrysum stoechas variety olonnense. Chem. Nat. Comp. 40 (2), 118–121.

Les, F., Venditti, A., Cásedas, G., Frezza, C., Guiso, M., Sciubba, F., Serafini, M., Bianco, A., Valero, M.S., López, V., 2017. Everlasting flower (Helichrysum stoechas Moench) as a potential source of bioactive molecules with antiproliferative, antioxidant, antidiabetic and neuroprotective properties. Indus. Crops and Prod. 108, 295–302.

Li, C., Yuan, S., Jiang, F., Xie, Y., Guo, Y., Yu, H., Cheng, Y., Qian, H., Yao, W., 2020. Degradation of fluopyram in water under ozone enhanced microbubbles: Kinetics, degradation products, reaction mechanism, and toxicity evaluation. Chemosphere 258, 127216.

Lourens, A.C.U., Viljoen, A.M., Heerden, F.R.V., 2008. South African Helichrysum species: A review of the traditional uses, biological activity and phytochemistry. J. Ethnopharmacol. 119, 630–652.

Maggio, A., Bruno, M., Guarino, R., Senatore, F., Ilardi, V., 2016. Contribution to a Taxonomic Revision of the Sicilian Helichrysum Taxa by PCA Analysis of Their Essential-Oil Compositions. Chem. Biodivers. 13 (2), 151–159.

Mukherjee, P.K., Saha, K., Das, J., Pal, M., Saha, B.P., 1997. Studies on the Anti-inflammatory activity of Rhizomes of Nelumbo nucifera. Planta Med. 63, 367–369.

Roussis, V., Tsoukatou, M., Chinou, I., Harvala, C., 2002. Composition and antibacterial activity of the essential oils of two Helichrysum stoechas varieties growing in the Island of Crete. J. Essen. Oil Res. 14 (6), 459–461.

Sachan, N.K., Arif, M., Zaman, Yatindra, K.K., 2011. Anti-inflammatory, analgesic and antioxidant potential of the stem bark of Spondias mangifera Willd. Arch. Biol. Sci. Belgrade. 63 (2), 413–419.

Sajad, M., Zargan, J., Chawla, R., Umar, S., Sadaqat, M., Khan, H. A., 2009. 'Hippocampal neurodegeneration in experimental autoimmune encephalomyelitis (EAE): potential role of inflammation activated myeloperoxidase. Mol. Cell Biochem. 328, 183–188.

Shushni, S.M.A., Azam, F., Lindequist, U., 2013. Oxasetin from Lophiostoma sp. of the Baltic Sea: identification, in silico binding mode prediction and antibacterial evaluation against fish pathogenic bacteria. Nat. Prod. Commun. 8 (9), 1223–1226.

Sobhy, E.A., El-Feky, S.S., 2007. Chemical constituents and antimicrobial activity of Helichrysum stoechas. Asian J. Plant Sci. 6 (4), 692–695.

Sripriya, N., M, R.K., N, A.K., S, B., N.K., U.P., 2019. In silico evaluation of multispecies toxicity of natural compounds. Drug Chem. Toxicol. 1–7.

Tsoukatou, M., Roussis, V., Chinou, I., Petrakis, P.V., Ortiz, A., 1999. Chemical composition of the essential oils and headspace samples of two Helichrysum species occurring in Spain. J. Essen. Oil Res. 11 (4), 511–516.

Tutin, T.G., Heywood, V.H., Burges, N.A., Moore, D.M., Valentine, D.H., Walters, S.M., Webb, D.A., 1980. 1980. Cambridge University Press, Flora Eurpaea.

Vernin, G., Poite, J.C., 1998. GC/MS analysis of volatile components of everlasting (*Helichrysum stoechas* L.) essential oil. J. Essential Oil Res. 10 (5), 553–557.

Williams, S., Bledsoe, R.K., Collins, J.L., Boggs, S., Lambert, M.H., Miller, A.B., Moore, J., McKee, D.D., Moore, L., Nichols, J.,

Parks, Watson, M., Wisely, B., Willson, T.M., 2003. X-ray crystal structure of the liver X receptor beta ligand binding domain: regulation by a histidine-tryptophan switch. J. Biol. Chem. 278 (29), 27138–27143.